Journal of Science and Transport Technology
Journal homepage: https://jstt.vn/index.php/en

Flexural performance of prestressed concrete I-shaped bridge girders exposed to hydrocarbon fire

Hung Viet Tran[1], Thang Ba Phung[2], Tung Duy Vu[2], Hang T.N. Nguyen[1,*]
[1]Faculty of Bridges and Roads, Hanoi University of Civil Engineering, 55 Giai Phong Street, Hanoi, Vietnam
[2]Faculty of Civil Engineering, University of Transport Technology, 54 Trieu Khuc Street, Hanoi, Vietnam

Article info
Type of article:
Original research paper

DOI:
https://doi.org/10.58845/jstt.utt.2025.en.5.1.61-76

***Corresponding author:**
Email address:
hangntn@huce.edu.vn

Received: 04/03/2025
Received in Revised Form: 20/03/2025
Accepted: 22/03/2025

Abstract: This study examines the flexural performance of identical I-shaped bridge girders with different prestressing arrangements and methods under fire conditions. A finite element model was developed to simulate the temperature evolution in the bridge girders exposed to fire. Temperature data from the model were used to assess the degradation in the ultimate strength of prestressing strands, as well as the reduction in flexural strength and the subsequent rating factor of both girders over time. The results reveal that the flexural capacity of the post-tensioned girder remained relatively stable for the first 90 minutes of fire exposure but gradually decreased thereafter. In contrast, the flexural strength of the pre-tensioned girder degraded more rapidly than that of the post-tensioned girder. Specifically, the pre-tensioned girder lost up to 51% of its initial flexural capacity, while the post-tensioned girder only lost 26% after four hours of exposure to a hydrocarbon fire. Additionally, the pre-tensioned girder lost its ability to carry the design live load after 100 minutes of fire exposure, whereas the post-tensioned girder retained this capacity for 190 minutes. The findings highlight that the prestressing arrangement is a crucial factor influencing the degradation of flexural capacity in prestressed girders under fire. Pre-tensioned girders, with strands located near the soffits, are significantly more vulnerable to strength loss compared to post-tensioned girders, which have cables positioned farther from the soffit. Additionally, fire intensity plays a critical role in determining the extent of degradation in the flexural strength of prestressed concrete bridge girders under fire conditions.
Keywords: Prestressed concrete; bridge engineering; flexural capacity; fire conditions; load rating; finite element method.

1. Introduction

Fire presents a significant hazard to bridges throughout their service life, and recent years have witnessed a growing number of fire-related incidents on bridges. Several notable cases of fire-induced bridge collapses have been documented in the literature [1-7]. One such example is the 2007 collapse of the MacArthur Maze I-80/880 interchange in Oakland, California. Other major incidents leading to bridge failures include the 2009 collapse of the I-75 expressway near Hazel Park, Michigan, the 2017 collapse of the Interstate 85 bridge in Atlanta, Georgia, the fire-induced collapse of the bridge over Tempe Town Lake, Arizona, in

2020, and a fire-related bridge collapse in Rome, Italy, in 2021.

Although the probability of a fire occurring on a bridge is lower than in commercial or industrial buildings, the economic and public losses resulting from such incidents can be substantial. These losses extend beyond the costs of retrofitting or rebuilding, also including expenses related to diverting traffic to alternative routes for extended periods, which can severely impact regional traffic flow and quality [1, 4, 5, 8]. A comprehensive understanding of how bridges perform under fire conditions is essential for developing effective repair strategies for fire-exposed structures, thereby minimizing both economic and public disruptions.

Over the past two decades, the frequency of fire incidents involving bridges has increased, leading to a growing body of research investigating how bridges behave when exposed to fire. These studies have primarily focused on two key areas: (1) evaluating the residual strength of fire-exposed bridges [2-4, 9-18], and (2) assessing fire hazards to bridges while developing inspection and repair strategies [1, 4-8, 19-24].

In the realm of concrete bridge fire endurance, Zhang et al. [4] studied the behavior of prestressed concrete box bridge girders, while Timilsina and Yazdani [17] investigated a concrete bridge in Irving, Texas, after a real fire event in 2005 using theoretical modeling and in-situ testing. Their findings revealed that thermal effects could reduce the modulus of elasticity of the girders and deck slab by 10 to 75%. In 2018, Beneberu and Yazdani [18] conducted a full-scale study of one-span prestressed concrete girders exposed to a combined hydrocarbon pool fire and simulated live load. Among the three specimens, the two girders strengthened with carbon fiber-reinforced polymer (CFRP) but without fireproofing sustained severe damage. In contrast, the third girder, which was fireproofed, exhibited lower temperatures, preserving the integrity of the CFRP bonding. These studies collectively demonstrate that concrete bridges are highly vulnerable to extreme fire events.

Additionally, a review of the literature and bridge incidents by Zhang and Zhao [11] highlighted that although steel bridges are generally more susceptible to fire, concrete bridges can also suffer severe damage or even collapse when exposed to fire. Despite this, research on the behavior of concrete bridges under fire conditions remains limited. This gap in knowledge has led to delays in identifying effective repair strategies, contributing to both economic and public losses.

To address this research gap, the present study focuses on the flexural performance and load rating of prestressed concrete I-shaped bridge girders exposed to hydrocarbon fire, a type of fire commonly generated by oil or gas combustion. The selection of I-shaped girders is based on their widespread use in practice. Furthermore, to evaluate the impact of strand arrangement on the load rating of fire-exposed bridge girders, both pre-tensioned and post-tensioned girders were analyzed.

To achieve these objectives, a finite element (FE) model was developed using Abaqus [25] to determine the temperature distribution within the selected girders under fire conditions. Based on the temperature data obtained from the validated FE model, the degradation of material strength and moment resistance of the girders over time due to fire exposure was calculated using established assumptions and theories [26, 27]. The resulting degradation in flexural strength and load ratings of the girders as a function of fire exposure time was then determined and compared. Additionally, parametric studies were conducted to investigate the factors affecting the flexural strength of concrete bridge girders subjected to fire.

The FE analysis and theoretical calculations are presented in this paper. The findings provide valuable insights into the behavior of prestressed concrete bridge girders exposed to fire and can inform future assessments of real fire scenarios in I-shaped bridge girders. It is important to note that

the predicted temperature profiles and subsequent calculation results are applicable only in the absence of spalling. Indeed, explosive spalling of concrete under fire conditions is a highly complex phenomenon influenced by numerous factors, including the permeability of concrete, type of aggregate, moisture content, heating rate, applied load level, concrete age, curing conditions, and section properties. Given the many variables involved, this issue falls outside the scope of the present study. Therefore, spalling is not considered in this study, consistent with assumptions made in previous research involving normal-strength concrete structures with a compressive strength below 70 MPa [28-30]. It should be highlighted that, under fire conditions, if explosive spalling occurs, it exposes the inner concrete to direct fire, altering the temperature progression and causing a rapid increase in temperature compared to scenarios where spalling is absent.

2. Moment resistance of concrete members exposed to fire – Theoretical analysis

For a general T-section, when the neutral axis lies within the web, the nominal flexural resistance at room temperature can be determined using the force analysis presented in Fig 1, as outlined in the AASHTO LRFD Bridge Design Specifications [31]. The nominal flexural resistance can be expressed as:

$$M_n = A_{ps} f_{ps} (d_p - \frac{a}{2}) + 0.85 f_c^{'} (b - b_w) h_f (\frac{a}{2} - \frac{h_f}{2}) \quad (1)$$

where

A_{ps} is area of prestressing steel, mm^2

$f_{ps}=f_{pu}(1- k\frac{c}{d_p})$ is average stress in prestressing steel, MPa

d_p is distance from the extreme compression fiber to the centroid of prestressing steel, mm

c distance from extreme compression fiber to the neutral axis, mm

fpy is the yield stress of prestressing steel, MPa

fpu is the ultimate stress of prestressing steel, MPa

$f_c^{'}$ is design concrete compressive strength, MPa

b is the effective width of the flange, mm

b_w is web width, mm

$a=c\beta_1$ is the depth of the equivalent stress block, mm

h_f is compression flange depth, mm.

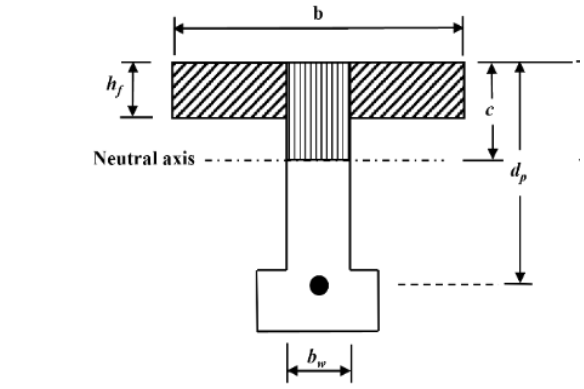

(a)

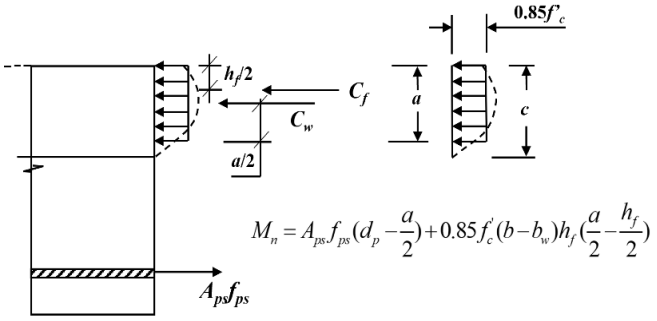

(b)

Fig 1. Force analysis to calculate moment resistance of an arbitrary section (a) an arbitrary section, (b) force analysis

If the neutral axis lies within the flange, the nominal moment resistance of the girder at room temperature is given by:

$$M_n = A_{ps} f_{ps} (d_p - \frac{a}{2}) \quad (2)$$

When a fire occurs, the strength of materials decreases with increasing temperatures. According to American design codes [27, 32], the retained moment capacity, where the neutral axis lies in the web and the flange, respectively, diminishes as follows:

$$M_{n\theta} = A_{ps} f_{ps\theta} (d_p - \frac{a_\theta}{2}) + 0.85 f_{c\theta}^{'} (b_\theta - b_{w\theta}) h_{f\theta} (\frac{a_\theta}{2} - \frac{h_{f\theta}}{2}) \quad (3)$$

$$M_{n\theta} = A_{ps} f_{ps\theta} (d_p - \frac{a_\theta}{2}) \quad (4)$$

in which θ denotes the effects of high temperatures. It should be noted that the codes

assume A_{ps} and d_p are not affected but f_{ps} is reduced to $f_{ps\theta}$ under elevated temperatures. For simply supported girder bridges, when fire occurs from the bottom, the depth of the equivalent stress block a (and also the depth of compression zone c) is reduced while the concrete strength at the top slab, f'_c, is generally not reduced because of its lower temperature [27]. Flexural failure can be presumed to occur when $M_{n\theta}$ is reduced to applied moment M. Therefore, fire resistance of structures in general depends on the level of load applied and the temperature-dependent strength of prestressing steel.

3. Investigated Girder properties

3.1. Geometric properties

In this study, an I-shaped cross section with a height of 1650 mm was selected as a case study to determine the flexural capacity and load rating of concrete bridge girders under fire conditions. This girder height is commonly used in simply supported bridges with a span length of 33 meters and is constructed using the semi-precast method. In this approach, the I-girder is prefabricated using either pretensioning or posttensioning techniques, then lifted onto the piers and abutments, with the deck slab cast in place to create a composite section.

Two 1650 mm high girders with identical concrete section properties but different strand arrangements and prestressing methods designated G-I33-Post and G-I33-Pre were used in this study. G-I33-Post refers to a bridge girder with an I-section and a 33 m span length, utilizing the posttensioning method. In contrast, G-I33-Pre denotes the same I33 girder but with a different strand arrangement, using the pretensioning method. The cross-sectional dimensions and strand arrangements of the two girders are shown in Fig 2.

As shown in Fig 2(a), G-I33-Post consists of four post-tension cable bundles, numbered 1 to 4. In contrast, G-I33-Pre is stressed with 52 pre-tensioned strands arranged in six rows, labeled Row 1 to Row 6, extending upward from the bottom of the girder (Fig 2(b)). A detailed strand numbering for G-I33-Pre is provided in Fig 3.

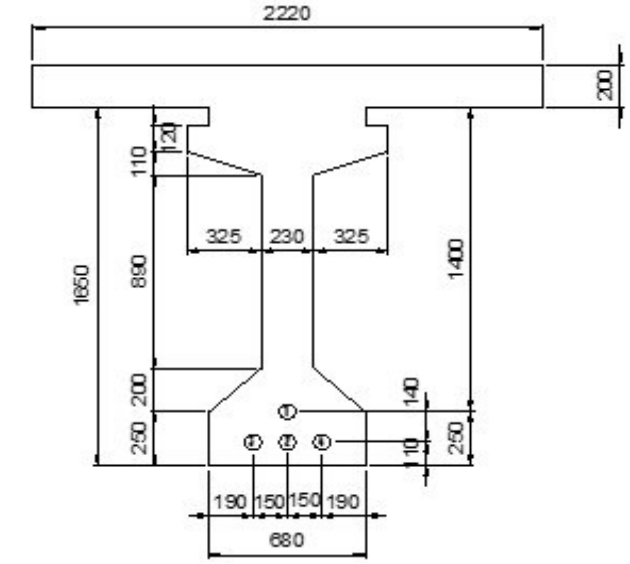

(a) G-I33-Post

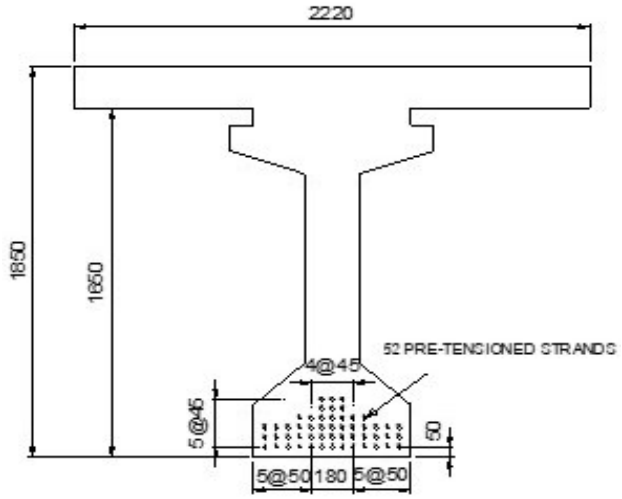

(b) G-I33-Pre

Fig 2. Cross section of investigated girders (after the deck slab is cast)

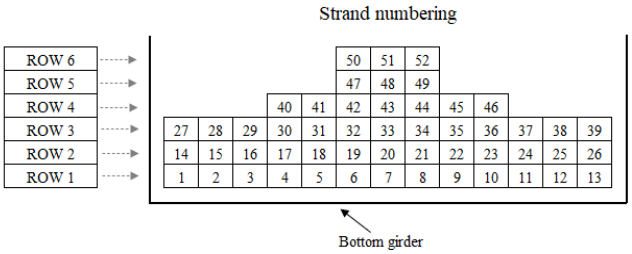

Fig 3. Strand numbering in G-I33-Pre

3.2. Material properties

The two precast I girders are made from concrete with a cylinder strength of 45 MPa, while the deck slab is constructed with concrete having a strength of 30 MPa. These concrete strengths are

commonly used in the bridge industry for both girders and bridge slabs. Each cable bundle in G-I33-Post consists of nine seven-wire, low-relaxation strands, each with a diameter of 15.2 mm, corresponding to a nominal area of 140 mm². In contrast, G-I33-Pre uses 52 pre-tensioned strands, each with a diameter of 12.7 mm and an area of 98.7 mm². The yield and ultimate strengths of all strands are 1670 MPa and 1860 MPa, respectively. During fabrication, each cable is subjected to a jacking stress of 75% of its ultimate strength. This prestressing process enhances the load-carrying capacity and increases the durability of the bridge girders throughout their service life.

4. Numerical modeling – heat transfer

4.1. Fire curves

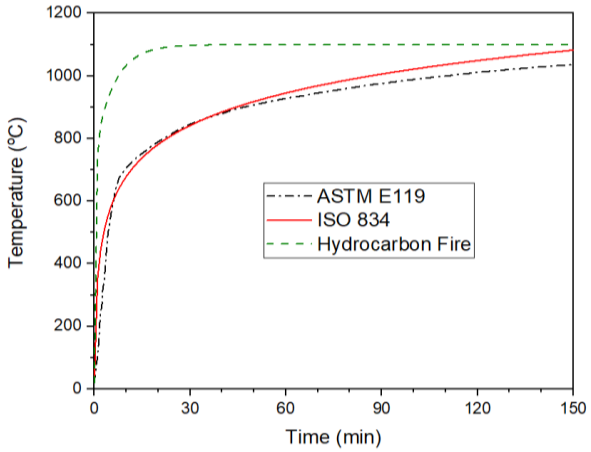

Fig 4. Standard fire curves vs. hydrocarbon fire

Heating curves illustrate the time-temperature relationship between the environment and the exposed surfaces of structural members during fire conditions. The ISO 834 heating curve, also known as the standard fire curve, is commonly used in fire tests to assess the fire resistance of structures, as specified in Eurocode 2 Part 1-2 [26]. In North America, the ASTM E119 [33] fire curve, which closely resembles the ISO 834 curve, is widely adopted. However, it is important to note that these curves represent severe fire conditions typically found in residential buildings and may not account for all possible fire scenarios, such as those caused by oil tanker fires in bridges and tunnels. In such cases, a hydrocarbon fire curve, specified in ASTM E1529-14a [34], is often used. Fig 4 compares these commonly used fire curves.

4.2. Modeling technique

In this study, concrete was modelled using 8-node linear heat transfer brick elements in a FE heat transfer model using Abaqus [25]. The concrete was divided into elements with a mesh size of 40 mm, which has been shown to capture temperature development in concrete structures under fire conditions with good accuracy [29, 35, 36]. The element mesh of investigated girders is shown in Fig 5.

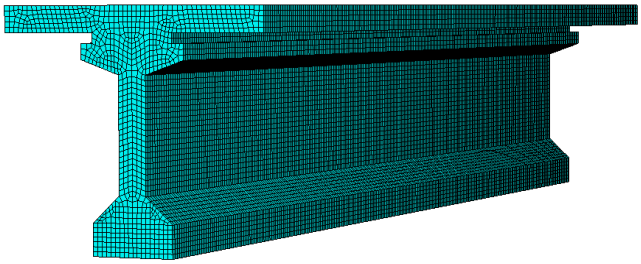

Fig 5. Element mesh

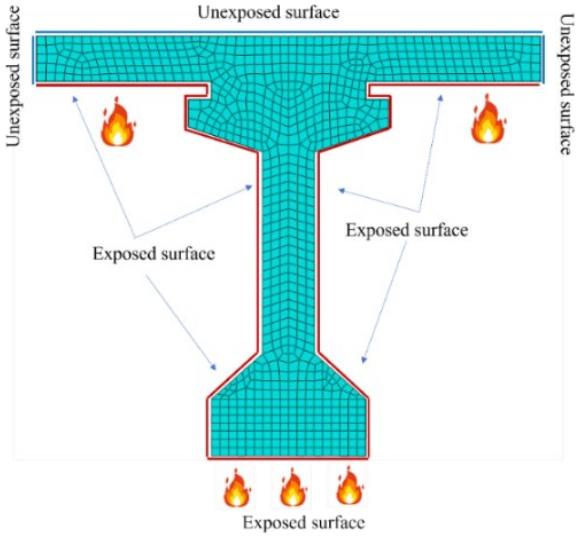

Fig 6. Thermal interaction

After fires occur, temperatures are transmitted to the concrete elements in two modes, i.e. convection and radiation. Heat is then transferred within the concrete molecules from higher temperature locations to lower temperature locations through conduction. In the FE heat transfer model, the two I-shaped girders were modelled in such a way that they interacted with fire sources at the three sides and the lower surface of the deck slab and with the natural environment (ambient temperature) at the upper

surface of the deck slab (Fig 6). Convective factors for the heated surfaces and nonheated surfaces were 25 and 10 W/m^{2}K, respectively, as recommended by Eurocode Part 1-2 [26]. For structures subjected to hydrocarbon fires, the convective factor will be taken as 50 W/m^{2}K [26]. The emissivity regarding concrete surface under fire conditions was 0.7 as suggested by Eurocode 2.

4.3. Thermal properties of concrete

To simulate heat transfer in concrete molecules, temperature-time-dependent properties of concrete including thermal conductivity and specific heat must be included in Abaqus. These properties are not constant but vary with increasing temperature [29]. In this study, the thermal properties of concrete were assumed following the recommended values in Eurocode 2 Part 1-2 as shown in Fig 7. It should be noted that in FE heat transfer model of concrete structures, the thermal properties of reinforcement are generally ignored as they have very little effect on heat transmission process in concrete. This is due to the relatively low steel or prestressing steel ratios in concrete structures. For instance, in the I-shaped girders investigated, this ratio is below 0.5%. Therefore, the temperature in strands can be assumed to be equal to the concrete temperature at the location of the reinforcement center. This assumption was also adopted in previous studies on the behavior of concrete structures exposed to fire [24, 29, 35, 37, 38].

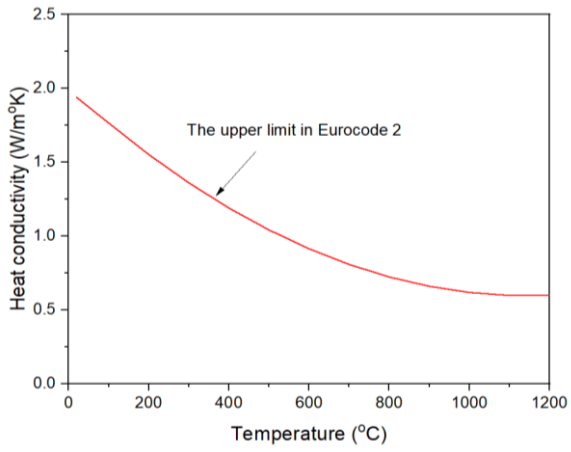

(a)

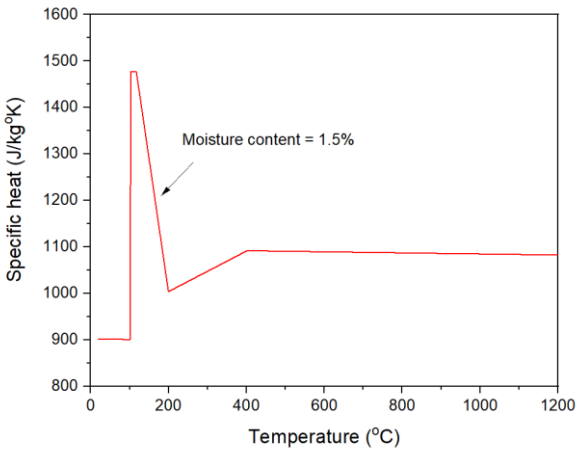

(b)

Fig 7. Thermal properties of concrete (a) Thermal conductivity, (b) Specific heat

4.4. Model validation

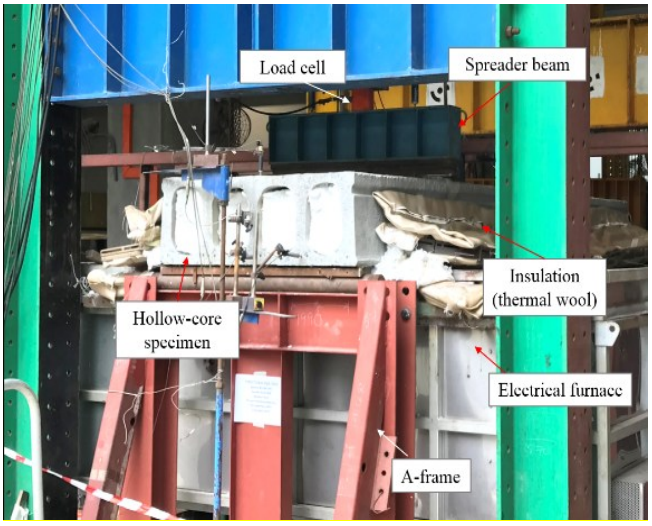

(a) Hollow-core slab in fire test

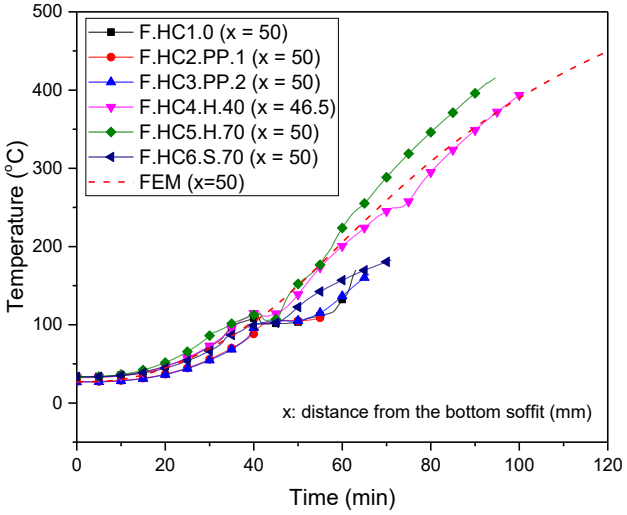

(b) Temperature comparison between the tests and the FE model (at x = 46.5 or 50 mm)

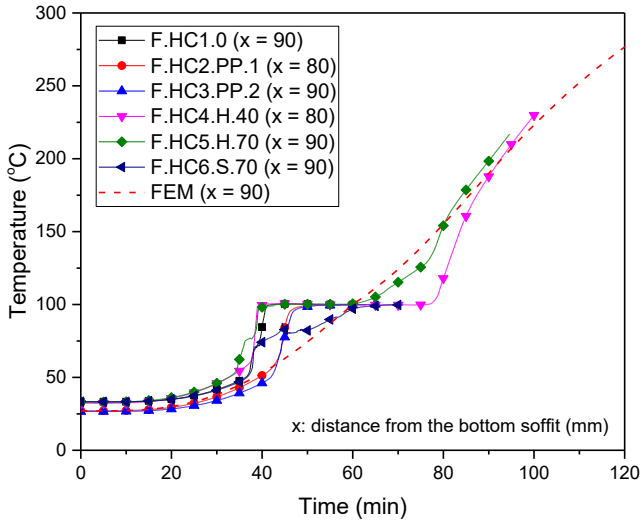

(c) Temperature comparison between the tests and the FE model (at x = 80 or 90 mm)

Fig 8. Verification of the FE heat transfer model using test data [35]

It should be noted that the similar heat transfer models were developed for prestressed concrete hollow-core slabs under fire conditions by the corresponding author and were verified using test data in previous studies [29, 35]. Fig 8 shows an example of the verification by comparing predicted temperatures from the numerical model with test data as shown in Nguyet *et al.* [35].

In this study, the FE model was further verified using predicted temperature data from Eurocode 2. As Eurocode 2 does not provide temperature development for I sections, a concrete rectangular beam was modelled. The developed FE model was then validated by comparing the temperature prediction results between the heat transfer model and Eurocode 2 Part 1-2 (Annex A) [26]. It should be noted that Eurocode 2 uses the standard fire curve ISO 834. Therefore, ISO 834 fire was employed in this validation instead of hydrocarbon fire. A rectangular beam with dimension of 800 x 500 x 5000 mm (height x width x length) subjected to ISO 834 fire (Fig 9) was modelled using the techniques and concrete thermal properties presented in Sections 4.2 and 4.3. Fig 10 shows the numerical results of temperature profiles in the beam at different times of fire exposure.

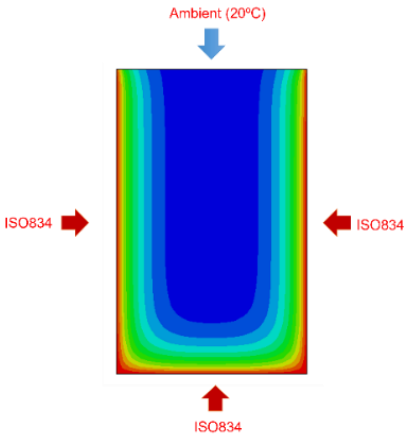

Fig 9. Thermal boundary conditions of an 800x500 mm rectangular beam subjected to ISO 834 fire

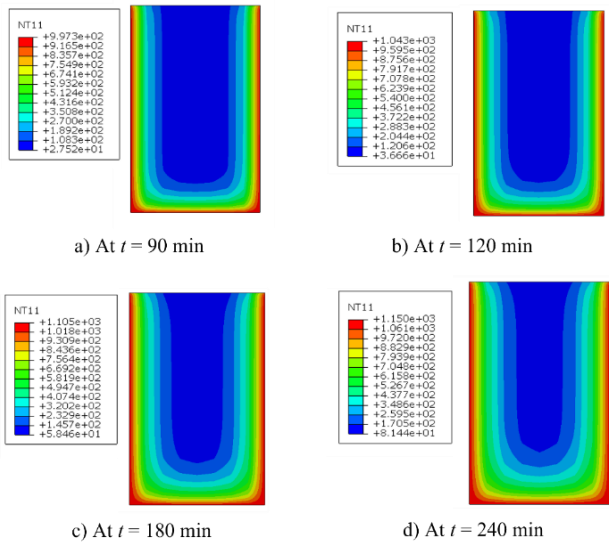

Fig 10. Temperature development in an 800 x 500 mm rectangular beam under ISO 834

Fig 10 illustrates that the temperature within the concrete beam gradually increased over time, with temperatures higher near the exposed surface compared to the middle region, which is consistent with expected trends. The validity of the FE model was confirmed by comparing the temperatures at various locations along the vertical centerline of the beam, obtained from the FE heat transfer model, with those suggested by Eurocode 2 (as shown in Fig 11). As seen in the comparison in Fig 11, the predicted temperatures from the FE model closely matched those recommended by Eurocode 2. These results demonstrate that the numerical model can accurately predict temperature development in fire-exposed concrete beams, thus

verifying the reliability of the FE model. Therefore, temperature predictions from the FE model can be confidently used to analyze heat transfer in concrete structures under fire conditions.

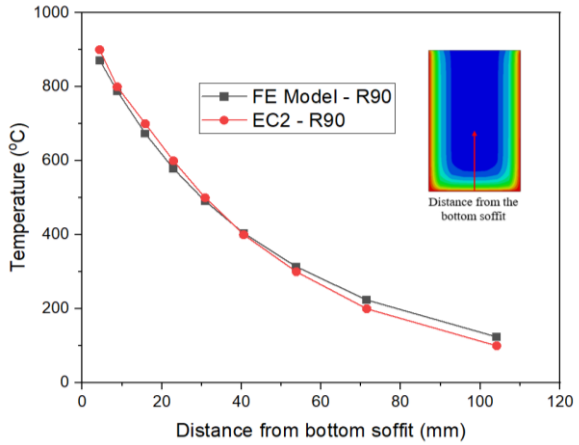

(a) At t = 90 min

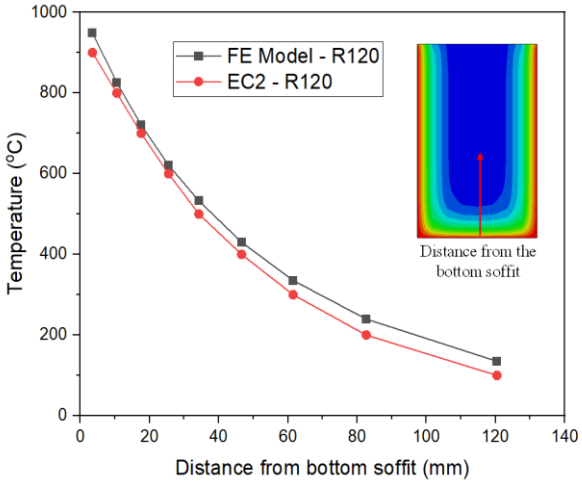

(b) At t = 120 min

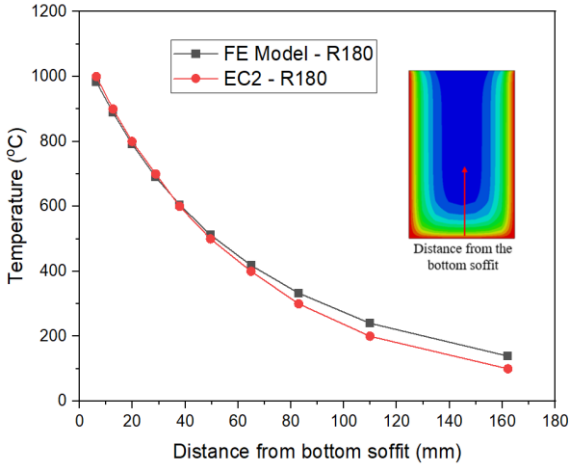

(c) At t = 180 min

Fig 11. Temperature profiles in an 800 x 500 mm rectangular beam under ISO 834

5. Results and discussion

5.1. Temperature development

G-I33-Post and G-I33-Pre were modeled under hydrocarbon fire conditions using the techniques, concrete thermal properties, and boundary conditions outlined in Sections 4.2 and 4.3. Since both girders have identical concrete section geometries, the temperature development is typically presented for G-I33-Post.

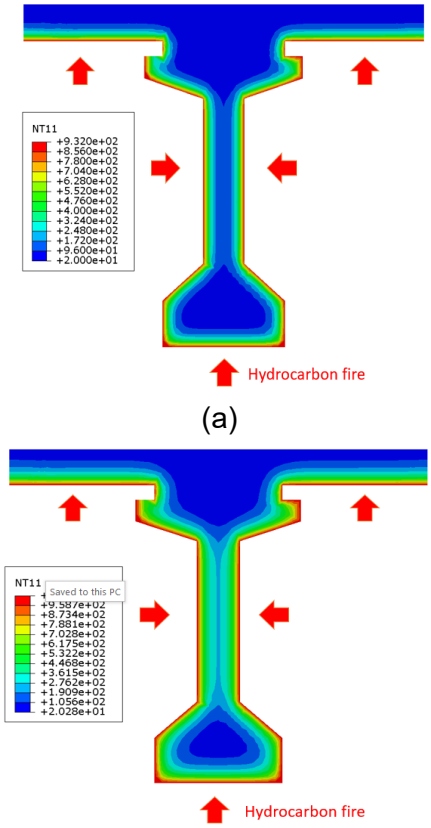

Fig 12. Temperature development across the cross-section of G-I33-Post (a) at 60 min, (b) at 120 min

Figs 12 and 13 illustrate the temperature evolution across the cross-section of G-I33-Post when exposed to a hydrocarbon fire. Similar to a concrete rectangular beam exposed to fire, the temperature in G-I33-Post was higher near the heated soffits compared to the inner regions. This is attributed to the low thermal conductivity and high specific heat of concrete, which, in contrast to metallic materials, slow the heat transfer process. Consequently, higher temperatures are observed near the soffits, while the inner regions remain

cooler. Additionally, Figs 12 and 13 show that the temperature in G-I33-Post increased over time, further validating the accuracy of the finite element model.

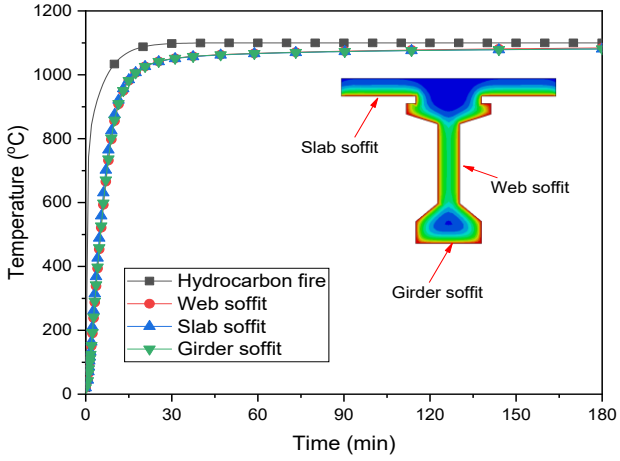

Fig 13. Evolution of concrete temperature at the exposed soffits of G-I33-Post under hydrocarbon fire

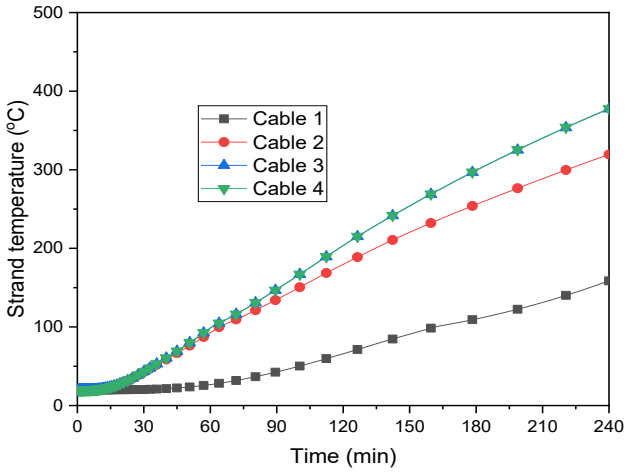

Fig 14. Strand temperature – G-I33-Post

To assess the degradation in flexural capacity of prestressed concrete structures under fire conditions, it is essential to determine the temperature in the prestressing strands. The flexural endurance of prestressed concrete members exposed to fire depends on the strength-temperature characteristics of the reinforcement [27]. Once the strand temperatures over time are determined, the moment capacity and the degradation in flexural strength can be defined. Fig 14 illustrates the temperature development in the four cables of G-I33-Post, while Fig 15 presents the average temperatures of the strands in the six rows, as shown in Fig 3. As observed, strand temperatures decreased as the distance from the bottom girder increased. Additionally, strand temperatures rose over time, further validating the accuracy of the FE model.

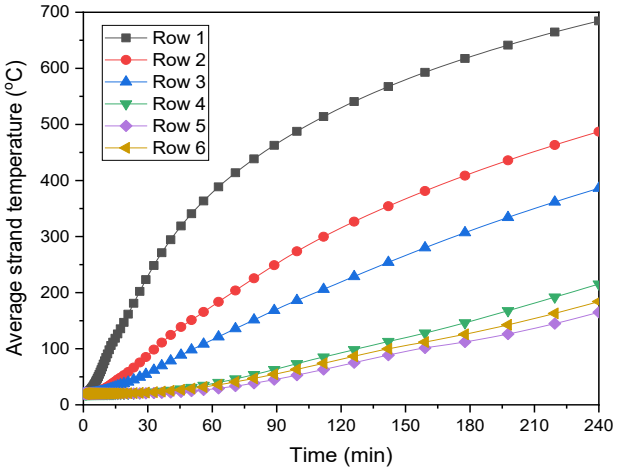

Fig 15. Strand temperature – G-I33-Pre

5.2. Degradation in moment resistance due to fire

The temperature measurements from the strands of the two investigated girders, shown in Fig 14 and 15, were used to assess the degradation of the ultimate strength of prestressing steel at high temperatures, based on ACI/TMS 216.1-14 [32], as shown in Fig 16. As can be seen in Fig 16, prestressing strands will lose 50 % of their ambient capacity at 420 °C. In laboratory fire tests, the tested structures can considered to fail if strand temperatures reach to this point [26, 32].

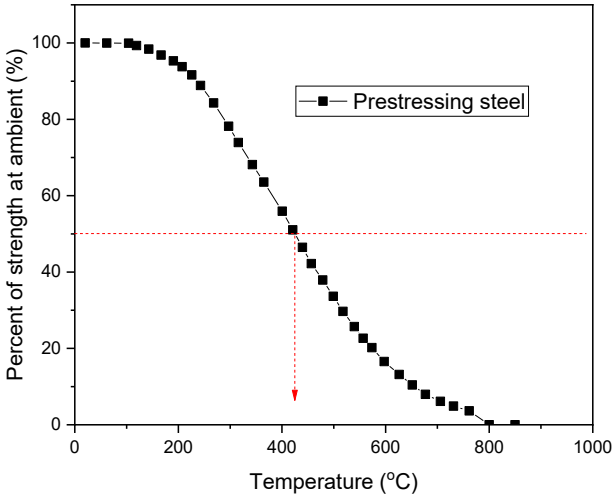

Fig 16. Ultimate strength of prestressing steel with elevated temperatures

Following the calculation principles outlined in Section 2, the flexural capacity of the two girders was determined for varying exposure times and plotted in Fig 17. Additionally, the ratio of the moment capacities of the two girders (with fire exposure time) to their initial moment capacities is presented in Fig 18.

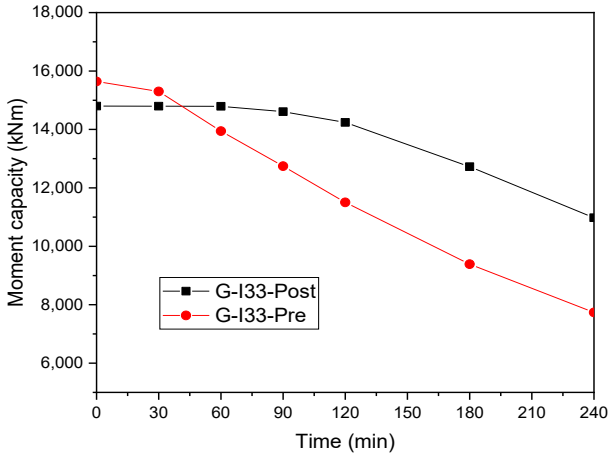

Fig 17. Moment capacity vs. time of G-I33-Post and G-I33-Pre under hydrocarbon fire

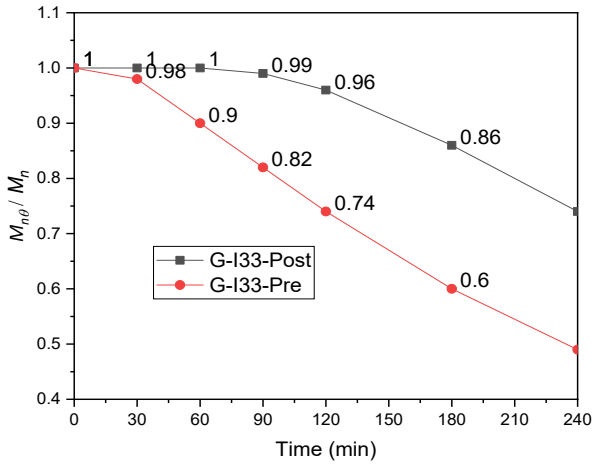

Fig 18. Degradation in flexural strength in G1-I33-Post and G2-I33-Pre under hydrocarbon fire

As shown in Fig 17, the post-tensioned concrete girder maintained its flexural capacity during the first 90 minutes of fire exposure. In contrast, the pre-tensioned concrete girder (G-I33-Pre) experienced a much faster reduction in flexural capacity compared to G-I33-Post. After 4 hours of fire exposure, G-I33-Pre lost up to 51% of its initial flexural capacity, which is a significantly greater reduction compared to the 26% loss observed in G-I33-Post at the same time (Fig 18). These results demonstrate that pre-tensioned girders with strands located near the girder soffits suffer a more substantial reduction in strength under fire conditions compared to post-tensioned girders, where the strands are positioned further from the soffits. The findings highlight the significant influence of prestressing steel arrangement on the flexural strength resistance of fire-exposed prestressed concrete bridge girders.

5.3. Rating factor of prestressed concrete bridge I-shaped girders under hydrocarbon fire

To determine whether the bridge girders exposed to fire can still support the design live load, the rating factor (RF) must be defined. According to TCVN 12882:2020 [39], the rating factor (RF) refers to the live load-carrying capacity of an existing bridge component. It is calculated as:

$$RF = \frac{C\text{-}DL}{LL} = \frac{HL}{LL} \quad (5)$$

where C is capacity of the component, LL is the live load effect, DL is dead load effect, and HL is the capacity to support live load. A rating factor (RF) greater than or equal to 1 indicates that the bridge component is capable of carrying the design live load, while an RF smaller than 1 signifies that the component cannot support the design live load.

Assuming that G-I33-Post or G-I33-Pre is placed in a superstructure with five identical girders spaced 2220 mm apart, with detailed cross sections of the overhang, barriers, and wearing surface as shown in Ba Danh and Minh Hung [40], the moment due to dead load and live load (HL93) effects is calculated following AASHTO [31], as shown in Fig 19. Rating factors over time of fire exposure are then computed and plotted in Fig 20. As observed in Fig 19, the effect of the dead load on both girders is more significant (6710 kNm, corresponding to 54%) compared to the effect of the live load (5634 kNm, corresponding to 46%). However, as shown in Fig 20, while G-I33-Post maintains the capacity to sustain HL93 up to 190 minutes of fire exposure, G-I33-Pre retains its live load-carrying capacity only for about 100 minutes, highlighting the vulnerability of pre-tensioned

girders under fire conditions.

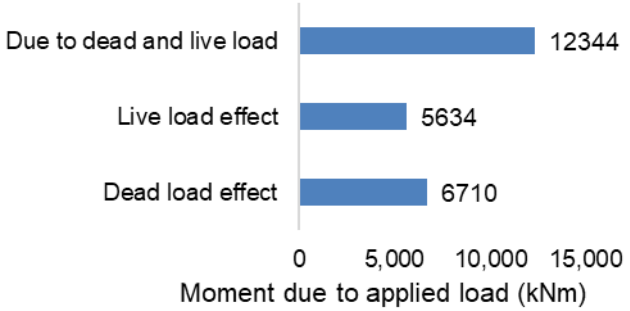

Fig 19. Moment due to load effect in G-I33-Pre and G-I33-Post

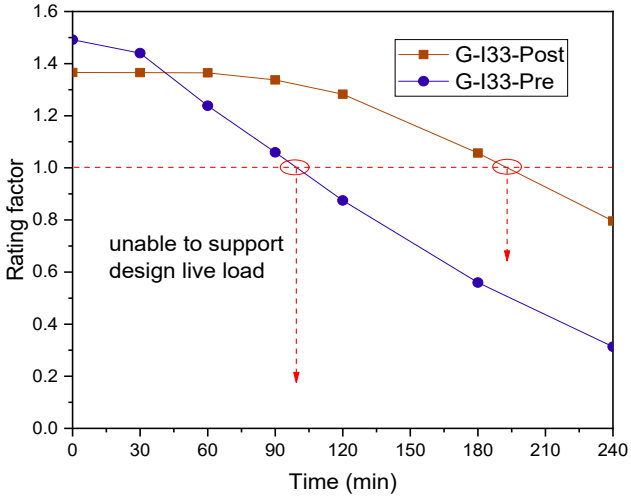

Fig 20. Rating factor of G-I33-Pre and G-I33-Post under hydrocarbon fire

6. Parametric studies

To study several parameters that affect the flexural response of prestressed concrete girders under fire conditions and to investigate whether the findings can be applied to other cross-sections of prestressed concrete girders, G-I33-Post is selected for parametric studies.

6.1. Effect of fire intensity

To investigate the effect of fire scenarios on the flexural resistance of prestressed concrete bridge girders under fire conditions, G-I33-Post was modeled and subjected to both ASTM E119 fire and hydrocarbon fire (Fig 4). The strand temperatures of G-I33-Post under ASTM E119 and hydrocarbon fire, as obtained from the FE model, are compared in Fig 21. As shown in Fig 21, after approximately 20 minutes of elevated temperatures, Cable 2 in G-I33-Post consistently exhibited a higher temperature than Cable 1 (Fig 21(a)). This can be attributed to their respective positions within the girder, with Cable 2 located closer to the fire-exposed bottom surface compared to Cable 1. Meanwhile, the temperatures in Cable 3 and Cable 4 remained nearly identical during the heating period (Fig 21(b)), as they are situated at the same level from the bottom soffit and are symmetric with respect to the girder's vertical centerline. Furthermore, since Cables 3 and 4 are positioned closer to the exposed side surface than Cable 2, their temperatures are higher than those of Cable 2, as shown in Figs 21(a) and (b). Additionally, all cables in G-I33-Post subjected to hydrocarbon fire exhibited higher temperatures compared to those exposed to ASTM E119 fire. This is because, during the first approximately 100 minutes of fire exposure, the temperature in a hydrocarbon fire is significantly higher than that of the ASTM E119 fire curve (Fig 4). As a result, the temperature in the concrete near the fire-exposed surfaces will be more severe in hydrocarbon fire than in ASTM E119 fire.

Temperature data from the FE heat transfer model were used to calculate the moment capacity of the girders over time. Fig 22 shows a comparison of the degradation in flexural strength of G-I33-Post exposed to both hydrocarbon and ASTM E119 fires. As shown in Fig 22, there were negligible changes in the flexural capacity of G-I33-Post after 90 minutes of exposure to either ASTM E119 or hydrocarbon fire. This indicates that, in the absence of spalling, the prestressed I-girder retained its initial flexural strength even after 90 minutes of exposure to fire scenarios. Additionally, as observed in Fig 22, the flexural strength of G-I33-Post remained consistent during the first 60 minutes of fire exposure in both scenarios. However, after 60 minutes, G-I33-Post subjected to hydrocarbon fire experienced a more rapid loss in flexural strength compared to the ASTM E119 fire. It was observed that after 240 minutes of exposure to hydrocarbon fire, the G-I33 girder lost 26% of its initial flexural capacity, while the girder exposed to

ASTM E119 fire lost only 21%. This demonstrates the significant role that fire intensity plays in the fire-related flexural resistance of prestressed concrete bridge girders.

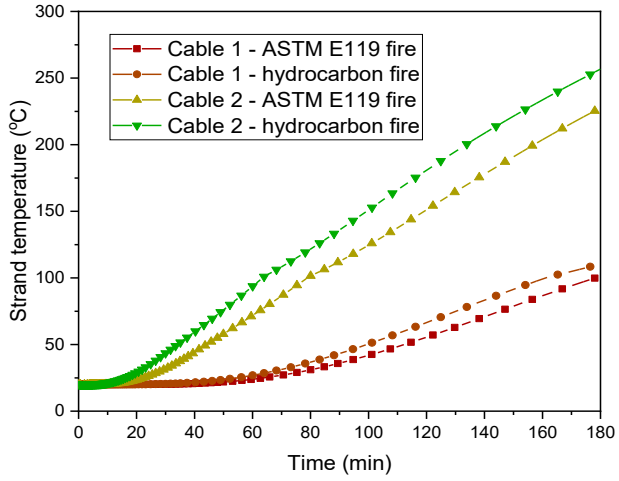

(a) Cables 1 & 2

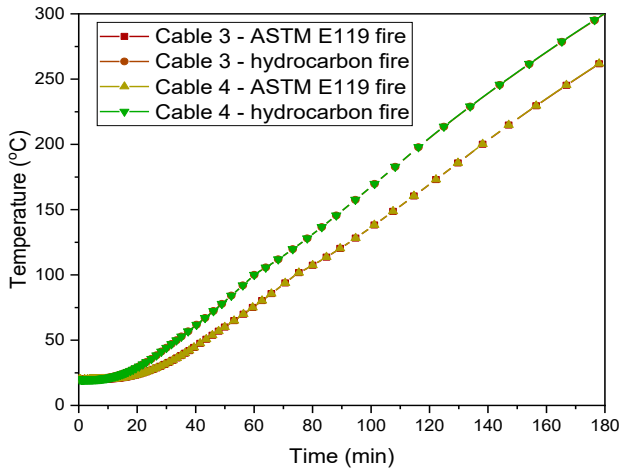

(b) Cables 3 & 4

Fig 21. Comparison of temperature development at the centroid of strand cables under ASTM E119 and hydrocarbon fire

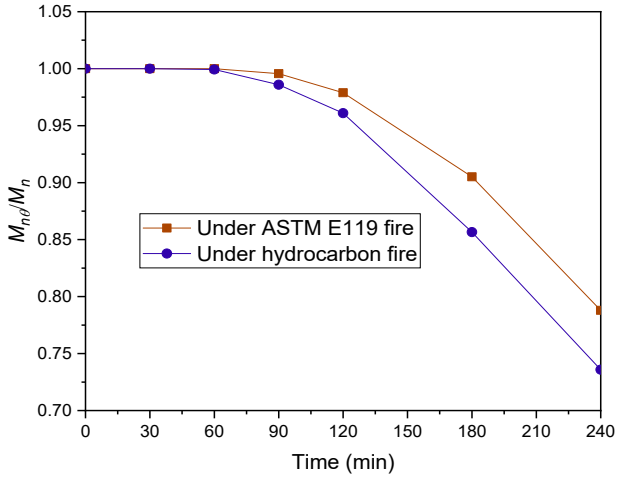

Fig 22. Comparison of the degradation in flexural strength of G-I33-Post under ASTM E119 and hydrocarbon fire

6.2. Effect of girder geometry

To examine the effect of girder dimensions on the reduction in flexural capacity of prestressed concrete bridge girders, two I-girders commonly used for simply supported bridges, with span lengths of 25 and 20 meters, namely G-I25-Post and G-I20-Post, respectively, were employed. The two girders were also modeled to be exposed to hydrocarbon fire for up to 4 hours, and the reductions in their flexural resistance at specific times were compared to those of G-I33-Post. The detailed geometric properties of G-I25-Post and G-I20-Post are shown in Fig 23. It should be noted that all three girders had similar steel arrangements, including the number of cables and the distances from the strand cables to the exposed soffits. Similar to G-I25-Post, the other two girders also contained four prestressing cables. However, each cable in G-I25-Post comprised 9 strands, while each cable in G-I20-Post consisted of 7 strands. All strands in G-I25-Post and G-I20-Post were seven-wire, low-relaxation types with a strand diameter of 12.7 mm (strand area of 98 mm²) and an ultimate strength of 1860 MPa. The concrete properties of G-I20-Post and G-I25-Post were identical to those of G-I33-Post.

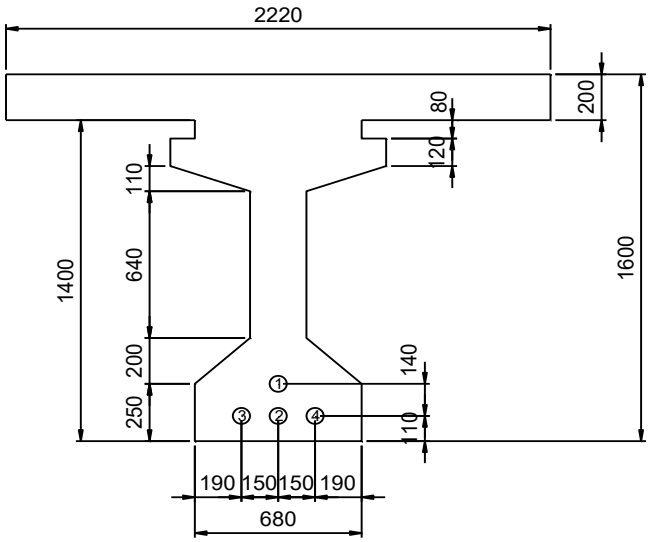

(a) G-I25-Post

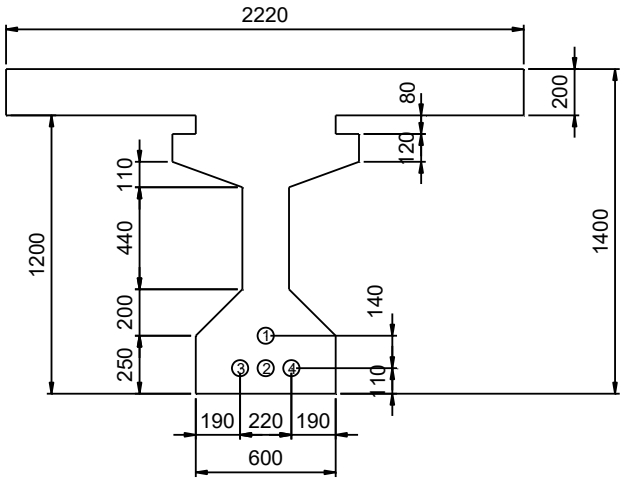

(b) G-I20-Post

Fig 23. Geometric properties of G-I25-Post and G-I20-Post

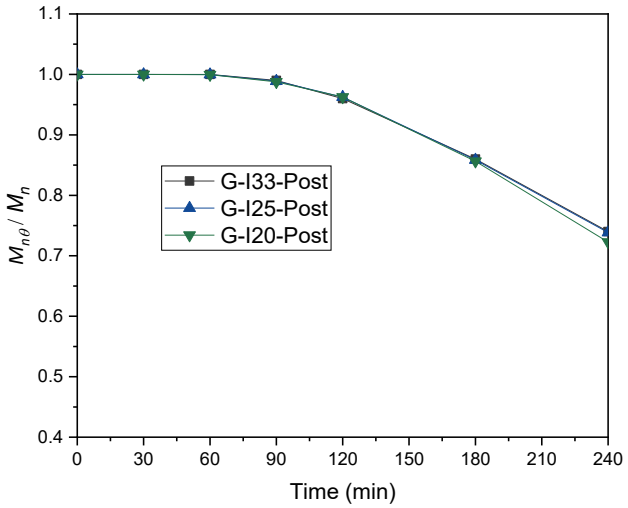

Fig 24. Comparison of the degradation in flexural strength of three post-tensioned girders subjected to hydrocarbon fire

Temperature development in the fire-exposed G-I25-Post and G-I20-Post was determined from the FE model. Their moment resistance at different fire exposure times was then calculated. The reduction in flexural strength of the two girders was compared to that of G-I33-Post, and the results are shown in Fig 24. The findings indicate that the degradation in flexural strength of the three girders was nearly identical at the same exposure times. This similarity can be attributed to the fact that all three girders had cables positioned at similar distances from the heated surfaces, resulting in comparable temperature developments in the strand cables over time. Consequently, the strength reductions in the prestressing cables at different times were relatively similar, regardless of the girder's geometry, leading to comparable degradations in flexural capacity. This part of the study, along with the results presented in Section 5.2, suggests that the steel arrangement, rather than the girder dimensions, determines the percentage reduction in flexural strength of prestressed concrete I-girders under fire conditions.

7. Conclusion

A study was conducted to investigate the flexural resistance and load rating factor of pre-tensioned and post-tensioned concrete I-shaped girders in bridge structures exposed to hydrocarbon fire. Finite element modeling was employed to determine the temperature variations in the girders under fire conditions. Analytical calculations were then carried out to evaluate the degradation in flexural strength and load rating of the girders during fire exposure. Based on the finite element and analytical results from this study, the following conclusions can be drawn

- The development of temperatures in prestressed concrete girders under fire conditions can be effectively predicted using the finite element method.

- Post-tensioned concrete I-shaped bridge girders, similar to those investigated in this study, can withstand up to 90 minutes of hydrocarbon fire exposure without significant loss in their flexural capacity. Beyond this period, the flexural resistance of these girders starts to degrade.

- Pre-tensioned bridge girders with strands positioned close to the exposed soffits experience a greater loss of flexural strength compared to post-tensioned girders, where the cables are located further from the soffits, under fire conditions. For example, G-I33-Pre, a pre-tensioned girder with strands near the soffit, lost 51% of its initial flexural capacity after 4 hours of hydrocarbon fire exposure. In contrast, the post-tensioned girder only experienced a 26% reduction. These results highlight that the

arrangement of the prestressing steel significantly influences the reduction in flexural capacity of concrete bridge girders under fire conditions.

- Pre-tensioned and post-tensioned I-shaped bridge girders, similar to those investigated in this study, would lose the capacity to support live loads after 100 and 190 minutes of fire exposure, respectively.

- The parametric studies show that fire intensity significantly affects the reduction in the flexural capacity of prestressed concrete bridge girders under fire conditions. Additionally, the steel arrangement, rather than the girder dimensions, determines the percentage reduction in the flexural strength of prestressed concrete I-girders under fire conditions.

- The findings of this study offer valuable insights for evaluating the flexural capacity and developing effective retrofit strategies for prestressed concrete I-shaped bridge girders exposed to fire.

Acknowledgement

This research is funded by the Ministry of Education and Training under grand number B2023-XDA-02.

References

[1]. M.Z. Naser, V.K.R. Kodur. (2015). A probabilistic assessment for classification of bridges against fire hazard. *Fire Safety Journal*, 76, 65-73.

[2]. E.M. Aziz, V.K. Kodur, J.D. Glassman, M.E.M. Garlock. (2015). Behavior of steel bridge girders under fire conditions. *Journal of Constructional Steel Research*, 106, 11-22.

[3]. E. Aziz, V. Kodur. (2013). An approach for evaluating the residual strength of fire exposed bridge girders. *Journal of Constructional Steel Research*, 88, 34-42.

[4]. G. Zhang, V. Kodur, J. Xie, S, He, W. Hou. (2017). Behavior of prestressed concrete box bridge girders under hydrocarbon fire condition. *Procedia Engineering*, 210, 449-455.

[5]. M. Garlock, I. Paya-Zaforteza, V. Kodur, L. Gu. (2012). Fire hazard in bridges: Review, assessment and repair strategies. *Engineering Structures*, 35, 89-98.

[6]. V.K.R. Kodur, M.Z. Naser. (2013). Importance factor for design of bridges against fire hazard. *Engineering Structures*, 54, 207-220.

[7]. W. Wright et al. (2013). Highway bridge fire hazard assessment. NCHRP 12. *Virginia Polytechnic Institute*.

[8]. V. Kodur, L. Gu, M.E.M. Garlock. (2010). Review and assessment of fire hazard in bridges. *Transportation Research Record: Journal of the Transportation Research Board*. 2172(1), 23-29.

[9]. W.L. Moore. (2008). Performance of fire-damaged prestressed concrete bridges. *Missouri University of Science and Technology*.

[10]. H. Saglik, A. Chen, R. Ma. (2022). Performance of bolted splice connection in I-girder composite bridges under tanker fire. *Journal of Constructional Steel Research*, 199, 107590.

[11]. G. Zhang, X. Zhao, Z. Lu, C. Song, X. Li, C. Tang. (2022). Review and discussion on fire behavior of bridge girders. *Journal of Traffic and Transportation Engineering*, 9(3), 422-446.

[12]. J. Alos-Moya, I. Paya-Zaforteza, M.E.M. Garlock, E. Loma-Ossorio, D. Schiffner, A. Hospitaler. (2014). Analysis of a bridge failure due to fire using computational fluid dynamics and finite element models. *Engineering Structures*, 68, 96-110.

[13]. Z. Zhang, T. Guo, S. Wang, J. Liu, L. Wang. (2021). Experimental study on post-fire properties of steel wires of bridge suspender. *Structures*, 33, 1252-1262.

[14]. X. Liu, C. Yu, W. Quan, L. Chen. (2019). Inspection, materials testing and field testing of a prestressed concrete box bridge after fire exposure. *Fire Safety Journal*, 108, 102852.

[15]. A.F. Izzet, N. Oukaili, N.A. Harbi. (2021). Post-fire serviceability and residual strength of composite post-tensioned concrete T-beams. *SN Applied Sciences*, 3(2), 1-25.

[16]. A.H. Varma et al. (2021). Post-Fire

Assessment of Prestressed Concrete Bridges in Indiana. *Purdue University. Joint Transportation Research Program: Purdue University*.

[17]. S. Timilsina, N. Yazdani, E. Beneberu. (2021). Post-fire analysis and numerical modeling of a fire-damaged concrete bridge. *Engineering Structures*, 244, 112764.

[18]. E. Beneberu, N. Yazdani. (2018). Performance of CFRP-strengthened concrete bridge girders under combined live load and hydrocarbon fire. *Journal of Bridge Engineering*, 23(7), 04018042.

[19]. J. Schumacher. (2016). Assessment of Bridge-Structures Under Fired Impact: A Case Study Approach. *University of Rhode Island*.

[20]. C. Jeoung et al. (2014). Bridge fire risk assessment on the highway in South Korea. *Advanced Materials Research. Trans Tech Publ*.

[21]. V.K. Kodur, M.Z. Naser. (2021). Classifying bridges for the risk of fire hazard via competitive machine learning. *Advances in Bridge Engineering*, 2(1), 1-12.

[22]. J. Albrektsson et al. (2011). Assessment of concrete structures after fire. *SP Technical Research Institute of Sweden*.

[23]. R.B. Stoddard. (2004). Inspection and repair of a fire damaged prestressed girder bridge. *Pittsburgh: International Bridge Conference*.

[24]. V.K. Kodur, E.M. Aziz, M.Z. Naser. (2017). Strategies for enhancing fire performance of steel bridges. *Engineering Structures*, 131, 446-458.

[25]. A.V. Simulia. (2014). 6.14 Documentation. ABAQUS (2014) Analysis User's Manual, Version 6.14. *Dassault Systemes*.

[26]. The European Union. (2004). EN-1992-1-2, Eurocode 2: Design of concrete structures, in Part 1-2: General rules - Structural fire design.

[27]. A.H. Gustaferro, L.D. Martin. (1989). Design for fire resistance of precast prestressed concrete. *Prestressed Concrete Institute*.

[28]. P. Kumar, V.K.R. Kodur. (2021). Response of prestressed concrete beams under combined effects of fire and structural loading. *Engineering Structures*, 246, 113025.

[29]. H.T.N. Nguyen, K.-H. Tan. (2021). Shear response of deep precast/prestressed concrete hollow core slabs subjected to fire. *Engineering Structures*, 227, 111398.

[30]. W.Y. Gao, J.-G. Dai, J.G. Teng, G.M. Chen. (2013). Finite element modeling of reinforced concrete beams exposed to fire. *Engineering Structures*, 52, 488-501.

[31]. AASHTO. (2017). AASHTO LRFD Bridge Design Specifications. *2017, American Association of State Highway and Transportation Officials*.

[32]. American Concrete Institute. (2014). Code requirements for determining fire resistance of concrete and masonry construction assemblies. *ACI Farmington Hills, MI*.

[33]. ASTM. (2012). E119–12a. Standard test methods for fire tests of building construction and materials.

[34]. ASTM. (2014). ASTM-E1529-14a, Standard test methods for determining effects of large hydrocarbon pool fires on structural members and assemblies. *2014: West Conshohocken, PA*.

[35]. H.T.N. Nguyen, Y. Li, K.H. Tan. (2021). Shear behavior of fiber-reinforced concrete hollow-core slabs under elevated temperatures. *Construction and Building Materials*, 275, 121362.

[36]. H.T.N. Nguyen, K.H. Tan. (2018). Shear behavior of deep precast/prestressed concrete hollow core slabs at ambient and under fire conditions. *43rd Conference on Our World in Concrete & Structures, 2018, Singapore (Keynote paper).*

[37]. H.T.N. Nguyen. (2020). Shear behavior of deep precast/prestressed concrete hollow-core slabs with and without fibers at ambient and under fire conditions. *2020, Nanyang Technological University: PhD Thesis*.

[38]. J.V. Aguado et al. (2016). A 3D finite element

model for predicting the fire behavior of hollow-core slabs. *Engineering Structures,* 108, 12-27.

[39]. Ministry of Science and Technology. (2020). TCVN-12882:2020, Evaluation of Highway Bridge.

[40]. L.B. Danh, N.M. Hung. (2022). Principal design and calculation example of semi-precast prestressed reinforced concrete simply supported bridge girders according to TCVN 11823: 2017 (in Vietnamese). *2022, Vietnam: Construction Publisher*.